Production of WZ Events in $p\bar{p}$ Collisions at $\sqrt{s} = 1.96$ TeV and Limits on Anomalous WWZ Couplings

V. M. Abazov,[35] B. Abbott,[72] M. Abolins,[63] B. S. Acharya,[29] M. Adams,[50] T. Adams,[48] M. Agelou,[18] J.-L. Agram,[19] S. H. Ahn,[31] M. Ahsan,[57] G. D. Alexeev,[35] G. Alkhazov,[39] A. Alton,[62] G. Alverson,[61] G. A. Alves,[2] M. Anastasoaie,[34] T. Andeen,[52] S. Anderson,[44] B. Andrieu,[17] Y. Arnoud,[14] A. Askew,[48] B. Åsman,[40] A. C. S. Assis Jesus,[3] O. Atramentov,[55] C. Autermann,[21] C. Avila,[8] F. Badaud,[13] A. Baden,[59] B. Baldin,[49] P. W. Balm,[33] S. Banerjee,[29] E. Barberis,[61] P. Bargassa,[76] P. Baringer,[56] C. Barnes,[42] J. Barreto,[2] J. F. Bartlett,[49] U. Bassler,[17] D. Bauer,[53] A. Bean,[56] S. Beauceron,[17] M. Begel,[68] A. Bellavance,[65] S. B. Beri,[27] G. Bernardi,[17] R. Bernhard,[49,*] I. Bertram,[41] M. Besançon,[18] R. Beuselinck,[42] V. A. Bezzubov,[38] P. C. Bhat,[49] V. Bhatnagar,[27] M. Binder,[25] C. Biscarat,[41] K. M. Black,[60] I. Blackler,[42] G. Blazey,[51] F. Blekman,[33] S. Blessing,[48] D. Bloch,[19] U. Blumenschein,[23] A. Boehnlein,[49] O. Boeriu,[54] T. A. Bolton,[57] F. Borcherding,[49] G. Borissov,[41] K. Bos,[33] T. Bose,[67] A. Brandt,[74] R. Brock,[63] G. Brooijmans,[67] A. Bross,[49] N. J. Buchanan,[48] D. Buchholz,[52] M. Buehler,[50] V. Buescher,[23] S. Burdin,[49] T. H. Burnett,[78] E. Busato,[17] C. P. Buszello,[42] J. M. Butler,[60] J. Cammin,[68] S. Caron,[33] W. Carvalho,[3] B. C. K. Casey,[73] N. M. Cason,[54] H. Castilla-Valdez,[32] S. Chakrabarti,[29] D. Chakraborty,[51] K. M. Chan,[68] A. Chandra,[29] D. Chapin,[73] F. Charles,[19] E. Cheu,[44] D. K. Cho,[60] S. Choi,[47] B. Choudhary,[28] T. Christiansen,[25] L. Christofek,[56] D. Claes,[65] B. Clément,[19] C. Clément,[40] Y. Coadou,[5] M. Cooke,[76] W. E. Cooper,[49] D. Coppage,[56] M. Corcoran,[76] A. Cothenet,[15] M.-C. Cousinou,[15] B. Cox,[43] S. Crépé-Renaudin,[14] D. Cutts,[73] H. da Motta,[2] B. Davies,[41] G. Davies,[42] G. A. Davis,[52] K. De,[74] P. de Jong,[33] S. J. de Jong,[34] E. De La Cruz-Burelo,[32] C. De Oliveira Martins,[3] S. Dean,[43] J. D. Degenhardt,[62] F. Déliot,[18] M. Demarteau,[49] R. Demina,[68] P. Demine,[18] D. Denisov,[49] S. P. Denisov,[38] S. Desai,[69] H. T. Diehl,[49] M. Diesburg,[49] M. Doidge,[41] H. Dong,[69] S. Doulas,[61] L. V. Dudko,[37] L. Duflot,[16] S. R. Dugad,[29] A. Duperrin,[15] J. Dyer,[63] A. Dyshkant,[51] M. Eads,[51] D. Edmunds,[63] T. Edwards,[43] J. Ellison,[47] J. Elmsheuser,[25] V. D. Elvira,[49] S. Eno,[59] P. Ermolov,[37] O. V. Eroshin,[38] J. Estrada,[49] H. Evans,[67] A. Evdokimov,[36] V. N. Evdokimov,[38] J. Fast,[49] S. N. Fatakia,[60] L. Feligioni,[60] A. V. Ferapontov,[38] T. Ferbel,[68] F. Fiedler,[25] F. Filthaut,[34] W. Fisher,[66] H. E. Fisk,[49] I. Fleck,[23] M. Fortner,[51] H. Fox,[23] S. Fu,[49] S. Fuess,[49] T. Gadfort,[78] C. F. Galea,[34] E. Gallas,[49] E. Galyaev,[54] C. Garcia,[68] A. Garcia-Bellido,[78] J. Gardner,[56] V. Gavrilov,[36] P. Gay,[13] D. Gelé,[19] R. Gelhaus,[47] K. Genser,[49] C. E. Gerber,[50] Y. Gershtein,[48] D. Gillberg,[5] G. Ginther,[68] T. Golling,[22] N. Gollub,[40] B. Gómez,[8] K. Gounder,[49] A. Goussiou,[54] P. D. Grannis,[69] S. Greder,[3] H. Greenlee,[49] Z. D. Greenwood,[58] E. M. Gregores,[4] Ph. Gris,[13] J.-F. Grivaz,[16] L. Groer,[67] S. Grünendahl,[49] M. W. Grünewald,[30] S. N. Gurzhiev,[38] G. Gutierrez,[49] P. Gutierrez,[72] A. Haas,[67] N. J. Hadley,[59] S. Hagopian,[48] I. Hall,[72] R. E. Hall,[46] C. Han,[62] L. Han,[7] K. Hanagaki,[49] K. Harder,[57] A. Harel,[26] R. Harrington,[61] J. M. Hauptman,[55] R. Hauser,[63] J. Hays,[52] T. Hebbeker,[21] D. Hedin,[51] J. M. Heinmiller,[50] A. P. Heinson,[47] U. Heintz,[60] C. Hensel,[56] G. Hesketh,[61] M. D. Hildreth,[54] R. Hirosky,[77] J. D. Hobbs,[69] B. Hoeneisen,[12] M. Hohlfeld,[24] S. J. Hong,[31] R. Hooper,[73] P. Houben,[33] Y. Hu,[69] J. Huang,[53] V. Hynek,[9] I. Iashvili,[47] R. Illingworth,[49] A. S. Ito,[49] S. Jabeen,[56] M. Jaffré,[16] S. Jain,[72] V. Jain,[70] K. Jakobs,[23] A. Jenkins,[42] R. Jesik,[42] K. Johns,[44] M. Johnson,[49] A. Jonckheere,[49] P. Jonsson,[42] A. Juste,[49] D. Käfer,[21] S. Kahn,[70] E. Kajfasz,[15] A. M. Kalinin,[35] J. Kalk,[63] D. Karmanov,[37] J. Kasper,[60] D. Kau,[48] R. Kaur,[27] R. Kehoe,[75] S. Kermiche,[15] S. Kesisoglou,[73] A. Khanov,[68] A. Kharchilava,[54] Y. M. Kharzheev,[35] H. Kim,[74] T. J. Kim,[31] B. Klima,[49] J. M. Kohli,[27] M. Kopal,[72] V. M. Korablev,[38] J. Kotcher,[70] B. Kothari,[67] A. Koubarovsky,[37] A. V. Kozelov,[38] J. Kozminski,[63] A. Kryemadhi,[77] S. Krzywdzinski,[49] Y. Kulik,[49] A. Kumar,[28] S. Kunori,[59] A. Kupco,[11] T. Kurča,[20] J. Kvita,[9] S. Lager,[40] N. Lahrichi,[18] G. Landsberg,[73] J. Lazoflores,[48] A.-C. Le Bihan,[19] P. Lebrun,[20] W. M. Lee,[48] A. Leflat,[37] F. Lehner,[49,*] C. Leonidopoulos,[67] J. Leveque,[44] P. Lewis,[42] J. Li,[74] Q. Z. Li,[49] J. G. R. Lima,[51] D. Lincoln,[49] S. L. Linn,[48] J. Linnemann,[63] V. V. Lipaev,[38] R. Lipton,[49] L. Lobo,[42] A. Lobodenko,[39] M. Lokajicek,[11] A. Lounis,[19] P. Love,[41] H. J. Lubatti,[78] L. Lueking,[49] M. Lynker,[54] A. L. Lyon,[49] A. K. A. Maciel,[51] R. J. Madaras,[45] P. Mättig,[26] C. Magass,[21] A. Magerkurth,[62] A.-M. Magnan,[14] N. Makovec,[16] P. K. Mal,[29] H. B. Malbouisson,[3] S. Malik,[58] V. L. Malyshev,[35] H. S. Mao,[6] Y. Maravin,[49] M. Martens,[49] S. E. K. Mattingly,[73] A. A. Mayorov,[38] R. McCarthy,[69] R. McCroskey,[44] D. Meder,[24] A. Melnitchouk,[64] A. Mendes,[15] M. Merkin,[37] K. W. Merritt,[49] A. Meyer,[21] J. Meyer,[22] M. Michaut,[18] H. Miettinen,[76] J. Mitrevski,[67] J. Molina,[3] N. K. Mondal,[29] R. W. Moore,[5] G. S. Muanza,[22] M. Mulders,[49] Y. D. Mutaf,[69] E. Nagy,[15] M. Narain,[60] N. A. Naumann,[34] H. A. Neal,[62] J. P. Negret,[8] S. Nelson,[48] P. Neustroev,[39] C. Noeding,[23] A. Nomerotski,[49] S. F. Novaes,[4] T. Nunnemann,[25] E. Nurse,[43] V. O'Dell,[49] D. C. O'Neil,[5] V. Oguri,[3] N. Oliveira,[3] N. Oshima,[49] G. J. Otero y Garzón,[50] P. Padley,[76] N. Parashar,[58] S. K. Park,[31] J. Parsons,[67] R. Partridge,[73] N. Parua,[69] A. Patwa,[70] G. Pawloski,[76] P. M. Perea,[47] E. Perez,[18] P. Pétroff,[16] M. Petteni,[42] R. Piegaia,[1] M.-A. Pleier,[68]

P. L. M. Podesta-Lerma,[32] V. M. Podstavkov,[49] Y. Pogorelov,[54] A. Pompoš,[72] B. G. Pope,[63] W. L. Prado da Silva,[3] H. B. Prosper,[48] S. Protopopescu,[70] J. Qian,[62] A. Quadt,[22] B. Quinn,[64] K. J. Rani,[29] K. Ranjan,[28] P. A. Rapidis,[49] P. N. Ratoff,[41] S. Reucroft,[61] M. Rijssenbeek,[69] I. Ripp-Baudot,[19] F. Rizatdinova,[57] S. Robinson,[42] R. F. Rodrigues,[3] C. Royon,[18] P. Rubinov,[49] R. Ruchti,[54] V. I. Rud,[37] G. Sajot,[14] A. Sánchez-Hernández,[32] M. P. Sanders,[59] A. Santoro,[3] G. Savage,[49] L. Sawyer,[58] T. Scanlon,[42] D. Schaile,[25] R. D. Schamberger,[69] H. Schellman,[52] P. Schieferdecker,[25] C. Schmitt,[26] C. Schwanenberger,[22] A. Schwartzman,[66] R. Schwienhorst,[63] S. Sengupta,[48] H. Severini,[72] E. Shabalina,[50] M. Shamim,[57] V. Shary,[18] A. A. Shchukin,[38] W. D. Shephard,[54] R. K. Shivpuri,[28] D. Shpakov,[61] R. A. Sidwell,[57] V. Simak,[10] V. Sirotenko,[49] P. Skubic,[72] P. Slattery,[68] R. P. Smith,[49] K. Smolek,[10] G. R. Snow,[65] J. Snow,[71] S. Snyder,[70] S. Söldner-Rembold,[43] X. Song,[51] L. Sonnenschein,[17] A. Sopczak,[41] M. Sosebee,[74] K. Soustruznik,[9] M. Souza,[2] B. Spurlock,[74] N. R. Stanton,[57] J. Stark,[14] J. Steele,[58] K. Stevenson,[53] V. Stolin,[36] A. Stone,[50] D. A. Stoyanova,[38] J. Strandberg,[40] M. A. Strang,[74] M. Strauss,[72] R. Ströhmer,[25] D. Strom,[52] M. Strovink,[45] L. Stutte,[49] S. Sumowidagdo,[48] A. Sznajder,[3] M. Talby,[15] P. Tamburello,[44] W. Taylor,[5] P. Telford,[43] J. Temple,[44] M. Tomoto,[49] T. Toole,[59] J. Torborg,[54] S. Towers,[69] T. Trefzger,[24] S. Trincaz-Duvoid,[17] B. Tuchming,[18] C. Tully,[66] A. S. Turcot,[43] P. M. Tuts,[67] L. Uvarov,[39] S. Uvarov,[39] S. Uzunyan,[51] B. Vachon,[5] R. Van Kooten,[53] W. M. van Leeuwen,[33] N. Varelas,[50] E. W. Varnes,[44] A. Vartapetian,[74] I. A. Vasilyev,[38] M. Vaupel,[26] P. Verdier,[22] L. S. Vertogradov,[35] M. Verzocchi,[59] F. Villeneuve-Seguier,[42] J.-R. Vlimant,[17] E. Von Toerne,[57] M. Vreeswijk,[33] T. Vu Anh,[16] H. D. Wahl,[48] L. Wang,[59] J. Warchol,[54] G. Watts,[78] M. Wayne,[54] M. Weber,[49] H. Weerts,[63] M. Wegner,[21] N. Wermes,[22] A. White,[74] V. White,[49] D. Wicke,[49] D. A. Wijngaarden,[34] G. W. Wilson,[56] S. J. Wimpenny,[47] J. Wittlin,[60] M. Wobisch,[49] J. Womersley,[49] D. R. Wood,[61] T. R. Wyatt,[43] Q. Xu,[62] N. Xuan,[54] S. Yacoob,[52] R. Yamada,[49] M. Yan,[59] T. Yasuda,[49] Y. A. Yatsunenko,[35] Y. Yen,[26] K. Yip,[70] H. D. Yoo,[73] S. W. Youn,[52] J. Yu,[74] A. Yurkewicz,[69] A. Zabi,[16] A. Zatserklyaniy,[51] M. Zdrazil,[69] C. Zeitnitz,[24] D. Zhang,[49] X. Zhang,[72] T. Zhao,[78] Z. Zhao,[62] B. Zhou,[62] J. Zhu,[69] M. Zielinski,[68] D. Zieminska,[53] A. Zieminski,[53] R. Zitoun,[69] V. Zutshi,[51] and E. G. Zverev[37]

(D0 Collaboration)

[1]*Universidad de Buenos Aires, Buenos Aires, Argentina*
[2]*LAFEX, Centro Brasileiro de Pesquisas Físicas, Rio de Janeiro, Brazil*
[3]*Universidade do Estado do Rio de Janeiro, Rio de Janeiro, Brazil*
[4]*Instituto de Física Teórica, Universidade Estadual Paulista, São Paulo, Brazil*
[5]*University of Alberta, Edmonton, Alberta, Canada, Simon Fraser University, Burnaby, British Columbia, Canada, York University, Toronto, Ontario, Canada, and McGill University, Montreal, Quebec, Canada*
[6]*Institute of High Energy Physics, Beijing, People's Republic of China*
[7]*University of Science and Technology of China, Hefei, People's Republic of China*
[8]*Universidad de los Andes, Bogotá, Colombia*
[9]*Center for Particle Physics, Charles University, Prague, Czech Republic*
[10]*Czech Technical University, Prague, Czech Republic*
[11]*Institute of Physics, Academy of Sciences, Center for Particle Physics, Prague, Czech Republic*
[12]*Universidad San Francisco de Quito, Quito, Ecuador*
[13]*Laboratoire de Physique Corpusculaire, IN2P3-CNRS, Université Blaise Pascal, Clermont-Ferrand, France*
[14]*Laboratoire de Physique Subatomique et de Cosmologie, IN2P3-CNRS, Universite de Grenoble 1, Grenoble, France*
[15]*CPPM, IN2P3-CNRS, Université de la Méditerranée, Marseille, France*
[16]*Laboratoire de l'Accélérateur Linéaire, IN2P3-CNRS, Orsay, France*
[17]*LPNHE, IN2P3-CNRS, Universités Paris VI and VII, Paris, France*
[18]*DAPNIA/Service de Physique des Particules, CEA, Saclay, France*
[19]*IReS, IN2P3-CNRS, Université Louis Pasteur, Strasbourg, France, and Université de Haute Alsace, Mulhouse, France*
[20]*Institut de Physique Nucléaire de Lyon, IN2P3-CNRS, Université Claude Bernard, Villeurbanne, France*
[21]*III. Physikalisches Institut A, RWTH Aachen, Aachen, Germany*
[22]*Physikalisches Institut, Universität Bonn, Bonn, Germany*
[23]*Physikalisches Institut, Universität Freiburg, Freiburg, Germany*
[24]*Institut für Physik, Universität Mainz, Mainz, Germany*
[25]*Ludwig-Maximilians-Universität München, München, Germany*
[26]*Fachbereich Physik, University of Wuppertal, Wuppertal, Germany*
[27]*Panjab University, Chandigarh, India*
[28]*Delhi University, Delhi, India*
[29]*Tata Institute of Fundamental Research, Mumbai, India*
[30]*University College Dublin, Dublin, Ireland*

[31]*Korea Detector Laboratory, Korea University, Seoul, Korea*
[32]*CINVESTAV, Mexico City, Mexico*
[33]*FOM-Institute NIKHEF and University of Amsterdam/NIKHEF, Amsterdam, The Netherlands*
[34]*Radboud University Nijmegen/NIKHEF, Nijmegen, The Netherlands*
[35]*Joint Institute for Nuclear Research, Dubna, Russia*
[36]*Institute for Theoretical and Experimental Physics, Moscow, Russia*
[37]*Moscow State University, Moscow, Russia*
[38]*Institute for High Energy Physics, Protvino, Russia*
[39]*Petersburg Nuclear Physics Institute, St. Petersburg, Russia*
[40]*Lund University, Lund, Sweden, Royal Institute of Technology and Stockholm University, Stockholm, Sweden, and Uppsala University, Uppsala, Sweden*
[41]*Lancaster University, Lancaster, United Kingdom*
[42]*Imperial College, London, United Kingdom*
[43]*University of Manchester, Manchester, United Kingdom*
[44]*University of Arizona, Tucson, Arizona 85721, USA*
[45]*Lawrence Berkeley National Laboratory and University of California, Berkeley, California 94720, USA*
[46]*California State University, Fresno, California 93740, USA*
[47]*University of California, Riverside, California 92521, USA*
[48]*Florida State University, Tallahassee, Florida 32306, USA*
[49]*Fermi National Accelerator Laboratory, Batavia, Illinois 60510, USA*
[50]*University of Illinois at Chicago, Chicago, Illinois 60607, USA*
[51]*Northern Illinois University, DeKalb, Illinois 60115, USA*
[52]*Northwestern University, Evanston, Illinois 60208, USA*
[53]*Indiana University, Bloomington, Indiana 47405, USA*
[54]*University of Notre Dame, Notre Dame, Indiana 46556, USA*
[55]*Iowa State University, Ames, Iowa 50011, USA*
[56]*University of Kansas, Lawrence, Kansas 66045, USA*
[57]*Kansas State University, Manhattan, Kansas 66506, USA*
[58]*Louisiana Tech University, Ruston, Louisiana 71272, USA*
[59]*University of Maryland, College Park, Maryland 20742, USA*
[60]*Boston University, Boston, Massachusetts 02215, USA*
[61]*Northeastern University, Boston, Massachusetts 02115, USA*
[62]*University of Michigan, Ann Arbor, Michigan 48109, USA*
[63]*Michigan State University, East Lansing, Michigan 48824, USA*
[64]*University of Mississippi, University, Mississippi 38677, USA*
[65]*University of Nebraska, Lincoln, Nebraska 68588, USA*
[66]*Princeton University, Princeton, New Jersey 08544, USA*
[67]*Columbia University, New York, New York 10027, USA*
[68]*University of Rochester, Rochester, New York 14627, USA*
[69]*State University of New York, Stony Brook, New York 11794, USA*
[70]*Brookhaven National Laboratory, Upton, New York 11973, USA*
[71]*Langston University, Langston, Oklahoma 73050, USA*
[72]*University of Oklahoma, Norman, Oklahoma 73019, USA*
[73]*Brown University, Providence, Rhode Island 02912, USA*
[74]*University of Texas, Arlington, Texas 76019, USA*
[75]*Southern Methodist University, Dallas, Texas 75275, USA*
[76]*Rice University, Houston, Texas 77005, USA*
[77]*University of Virginia, Charlottesville, Virginia 22901, USA*
[78]*University of Washington, Seattle, Washington 98195, USA*

(Received 11 April 2005; published 29 September 2005)

We present results from a search for WZ production with subsequent decay to $\ell\nu\ell'\bar{\ell}'$ (ℓ and $\ell' = e$ or μ) using 0.30 fb^{-1} of data collected by the D0 experiment between 2002 and 2004 at the Fermilab Tevatron. Three events with WZ decay characteristics are observed. With an estimated background of 0.71 ± 0.08 events, we measure the WZ production cross section to be $4.5^{+3.8}_{-2.6}$ pb, with a 95% C.L. upper limit of 13.3 pb. The 95% C.L. limits for anomalous WWZ couplings are found to be $-2.0 < \Delta\kappa_Z < 2.4$ for form factor scale $\Lambda = 1$ TeV, and $-0.48 < \lambda_Z < 0.48$ and $-0.49 < \Delta g_1^Z < 0.66$ for $\Lambda = 1.5$ TeV.

DOI: 10.1103/PhysRevLett.95.141802 PACS numbers: 14.70.Fm, 13.40.Em, 13.85.Rm, 14.70.Hp

The $SU(2)_L \otimes U(1)_Y$ structure of the standard model (SM) Lagrangian implies that the electroweak gauge bosons W and Z interact with one another through trilinear and quartic vertices. As a consequence, the production cross section $\sigma(p\bar{p} \rightarrow WZ)$ depends on the WWZ gauge coupling shown in Fig. 1(a). The SM predicts that the strength of that coupling is $-e\cot\theta_W$, where e is the electric charge and θ_W is the weak mixing angle. More generally, excursions of the WWZ interactions from the SM can be described by an effective Lagrangian with parameters g_1^Z, λ_Z, and κ_Z [1]. This effective Lagrangian reduces to the SM Lagrangian when the couplings are set to their SM values $g_1^Z = \kappa_Z = 1$ and $\lambda_Z = 0$. Non-SM values of these couplings will increase σ_{WZ}. Therefore a measurement of the WZ production cross section provides a sensitive test of the strength of the WWZ interaction. This test also probes for low-energy manifestations of new physics, appearing at a higher mass scale, that complements searches to be carried out with future higher-energy accelerators [2].

A model-independent test for anomalous trilinear boson couplings using σ_{WZ} is unique among vector boson pair production processes in that WZ diagrams contain only WWZ, and not $WW\gamma$, vertices. Anomalous trilinear gauge boson coupling limits set using characteristics of W^+W^- production [3–9] are sensitive to both the $WW\gamma$ and WWZ couplings and must make an assumption [8,10] relating them. Furthermore, as production of the $W^\pm Z$ final state is unavailable at e^+e^- colliders [4–7], a hadron collider such as the Tevatron at Fermilab provides an unique opportunity for measurement of the WWZ coupling in isolation.

Using 90 pb^{-1} of $p\bar{p}$ collisions collected at $\sqrt{s} =$ 1.8 TeV during Run I (1992–1996), the D0 Collaboration established that $\sigma_{WZ} < 47$ pb at 95% C.L. From these data, D0 also set 95% C.L. limits $|g_1^Z - 1| <$ 1.63 and $|\lambda_Z| < 1.42$ for a form factor scale [1] $\Lambda =$ 1 TeV [9]. With a higher center-of-mass energy ($\sqrt{s} =$ 1.96 TeV) expected to increase the SM WZ production cross section to 3.7 ± 0.1 pb [11], more luminosity, and improved detectors, the Run II Tevatron program opens a new window for studies of WZ production. The CDF Collaboration recently announced a 15.2 pb upper limit at the 95% C.L. on the combined cross section for WZ and ZZ production [12]. However, no production cross section measurement for WZ has been reported by any experiment.

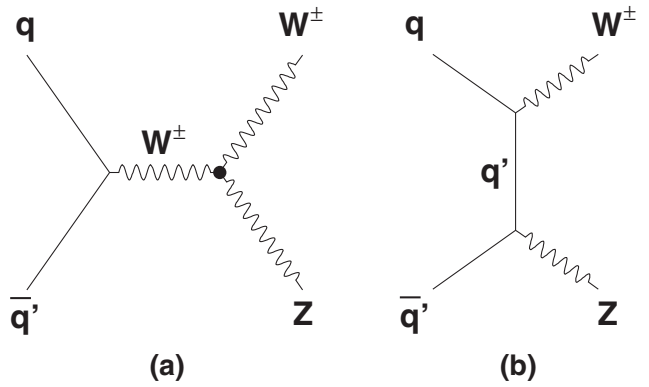

FIG. 1. Tree-level diagrams for WZ production in $p\bar{p}$ collisions. Diagram (a) contains the WWZ trilinear gauge coupling vertex.

We present the results of a search for WZ production with "trilepton" final states $\ell\nu\ell'\bar{\ell}'$ (ℓ and $\ell' = e$ or μ) using data collected by the D0 experiment from 2002–2004 at $\sqrt{s} = 1.96$ TeV. Requiring three isolated high transverse momentum (p_T) charged leptons and large missing transverse energy ($\not\!\!E_T$) to indicate the presence of a neutrino strongly suppresses backgrounds which mimic the WZ signal. However, branching ratios sum to only 1.5% for trilepton final states ($\mu\nu ee$, $e\nu\mu\mu$, $e\nu ee$, and $\mu\nu\mu\mu$). The WZ signal that we seek is distinct but rare.

The D0 detector [13,14] comprises several subdetectors and a trigger and data acquisition system. The central-tracking system consists of a silicon microstrip tracker (SMT) and a central fiber tracker (CFT) located within a 2 T superconducting solenoidal magnet. The SMT and CFT measure the locations of the collisions and the momenta of charged particles. The energies of electrons, photons, and hadrons, and the amount of $\not\!\!E_T$, is measured in three uranium or liquid-argon calorimeters, each housed in a separate cryostat [13]: a central section (CC) covering $|\eta| \leq 1.1$ and two end calorimeters (EC) extending coverage to $|\eta| \leq 4.2$, where η is the pseudorapidity. Scintillators between the CC and EC cryostats provide sampling of developing showers for $1.1 < |\eta| < 1.4$. A muon system [14] resides beyond the calorimetry, and consists of a layer of tracking detectors and scintillation trigger counters in front of 1.8 T toroidal magnets, followed by two similar layers behind the toroids. A three level trigger and data acquisition system uses information from the subdetectors to select ≈ 50 Hz of collisions for further "offline" reconstruction. Luminosity [15] is determined using scintillation counters located on each side of the interaction region and is calculated for each trigger.

The detector is well suited to identify signals with high-p_T leptons and missing transverse energy; see, for example, Ref. [16]. A combination of single and dilepton triggers was used for each channel. With at least three high-p_T charged leptons in the candidate events, the overall trigger efficiency for the WZ signal is nearly 100%. Integrated luminosities for the $ee\nu ee$, $\mu\nu ee$, $e\nu\mu\mu$, and $\mu\nu\mu\mu$ final states are 320 pb^{-1}, 290 pb^{-1}, 280 pb^{-1}, and 290 pb^{-1}, respectively, with a common uncertainty of 6.5% [15].

Electrons from W and Z boson decays are identified by their pattern of spatially isolated energy deposition in the calorimeter and by the presence of a matching track in the central-tracking system. The transverse energy of an elec-

tron, measured in the calorimeter, must satisfy $E_T > 15$ GeV.

A muon is identified by a pattern of hits in the scintillation counter and drift chamber system and must have a matching central track. Muon isolation is determined from an examination of the energy in calorimeter cells and the momenta of any additional tracks around the muon. Muons must have $p_T > 15$ GeV/c.

Missing transverse energy is determined from the negative of the vector sum of transverse energies of the calorimeter cells, adjusted for the presence of any muons identified above.

The WZ event selection requires at least three charged leptons that originate from a common interaction vertex and survive the electron or muon identification criteria outlined above. To associate reconstructed tracks with leptons unambiguously, they are required to be spatially separated. To select Z bosons and suppress backgrounds further, the invariant mass of a like-flavor lepton pair must fall within 71 GeV/c^2 to 111 GeV/c^2 for e^+e^- events, and 51 GeV/c^2 to 131 GeV/c^2 for $\mu^+\mu^-$ events, where the different mass windows correspond to the respective resolutions of the calorimeter and the central tracker. For the $e\nu ee$ and $\mu\nu\mu\mu$ channels, the lepton pair with invariant mass closest to the Z boson mass is chosen as the Z candidate. The $\not\!\!E_T$ is required to be greater than 20 GeV, consistent with a W boson decay. The transverse mass, although not used as a selection criterion, is calculated from the p_T of the unpaired third lepton and the $\not\!\!E_T$ [17]. Finally, to reject background from $t\bar{t}$ events, the absolute value of the vector sum of the transverse energy of the leptons, including the $\not\!\!E_T$, must be less than 50 GeV. This kinematic quantity [18] is equivalent to the p_T of the WZ system and takes its rejection against $t\bar{t}$ because that final state has two b-quark jets boosted against the leptons.

Applying all selection requirements leaves one $e\nu ee$ and two $\mu\nu\mu\mu$ candidates. Table I summarizes the kinematic properties of these events.

Signal acceptances include geometric and kinematic effects and are obtained using Monte Carlo samples produced with the PYTHIA event generator [20] followed by the GEANT-based [21] D0 detector-simulation program. Acceptances are calculated by counting the number of events that pass all selection criteria, except the lepton identification and track-matching requirements. The results are 0.283 ± 0.009, 0.279 ± 0.008, 0.287 ± 0.009, and 0.294 ± 0.008 for $e\nu ee$, $\mu\nu ee$, $e\nu\mu\mu$, and $\mu\nu\mu\mu$ final states, respectively.

Lepton-identification and central-track-matching efficiencies are estimated using samples of 21 000 $Z \to e^+e^-$ and 29 000 $Z \to \mu^+\mu^-$ events. One of the leptons from the Z boson decay is required to pass all lepton selection requirements. The other lepton is tested as to whether it passes the selection criteria. Both identification efficiencies and track-matching efficiencies are determined as functions of p_T and η. Average identification efficiencies are 0.929 ± 0.013 and 0.965 ± 0.008 for CC and EC electrons, respectively, and 0.940 ± 0.002 for muons. Track-matching efficiencies are 0.817 ± 0.002 for CC electrons, 0.674 ± 0.006 for EC electrons, and 0.950 ± 0.002 for muons. These efficiencies are folded into the WZ MC events used for acceptance calculations. The overall WZ acceptance times detection efficiencies are $(10.3 \pm 1.5)\%$, $(11.7 \pm 0.8)\%$, $(13.9 \pm 1.3)\%$, and $(16.3 \pm 1.8)\%$ for $e\nu ee$, $\mu\nu ee$, $e\nu\mu\mu$, and $\mu\nu\mu\mu$, respectively.

From the SM prediction for σ_{WZ} and the leptonic branching fractions of the W and Z bosons [22], we expect 0.44 ± 0.07, 0.45 ± 0.04, 0.53 ± 0.06, 0.62 ± 0.08 WZ events for the $e\nu ee$, $\mu\nu ee$, $e\nu\mu\mu$, and $\mu\nu\mu\mu$ final states, respectively. The total number of expected events is 2.04 ± 0.17. Quoted uncertainties include statistical and systematic contributions, the uncertainties in the W boson and Z boson branching fractions, as well as the 6.5% uncertainty in the integrated luminosity.

Among SM processes, WZ production is the dominant mechanism that results in events with a final state that includes three isolated leptons with large transverse momentum and with large $\not\!\!E_T$. The main backgrounds to WZ production come from $Z + X$ (X = hadronic jets, γ, or Z) events. In Z + jets events, a jet may be misidentified as an additional lepton. This background is estimated from data as follows. Events are selected using the same criteria as for the WZ sample, except that the requirement of the third lepton is dropped. The resulting ''dilepton + jets'' sample includes ee + jets, $\mu\mu$ + jets, and $e\mu$ + jets events. Probabilities for hadronic jets to mimic electrons and muons are determined, using multijet data, as a function

TABLE I. Kinematic properties of the three WZ candidates. Provided are the momentum four-vectors for the two leptons which constitute the Z boson candidate, the invariant mass formed from those two leptons, the momentum 4-vector of the charged lepton from the W boson decay, the components of the $\not\!\!E_T$, and the transverse mass computed from the third lepton and the $\not\!\!E_T$ [19]. The units are GeV, GeV/c, and GeV/c^2, as appropriate.

Final State	ℓ_Z				ℓ_Z					ℓ_W						
	p_x	p_y	p_z	E	p_x	p_y	p_z	E	$m_{\ell\ell}$	p_x	p_y	p_z	E	$\not\!\!E_{T_x}$	$\not\!\!E_{T_y}$	m_T
$e\nu ee$	−47.3	−25.9	292	297	13.3	37.6	111	118	91.9	45.3	−32.1	−16.5	57.9	−19.6	−23.5	72.3
$\mu\nu\mu\mu$	24.5	11.6	29.7	40.2	−38.7	−12.4	−17.1	44.1	82.1	−19.3	−16.7	101	105	24.1	19.8	56.4
$\mu\nu\mu\mu$	−15.1	19.9	24.4	35.0	20.2	−42.5	57.1	74.0	68.5	−21.9	−5.90	−16.4	28.0	34.8	25.4	62.5

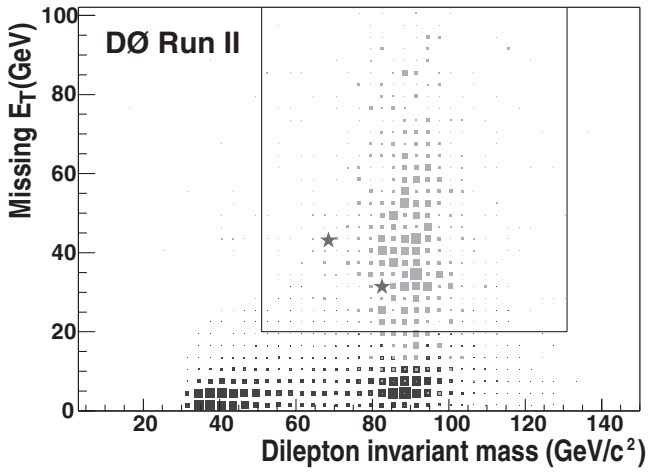

FIG. 2. $\not\!\!E_T$ vs dilepton invariant mass distribution for $\sim$200 fb^{-1} of simulated $WZ \to \mu\nu\mu\mu$ events (gray) and for 290 pb^{-1} of $\mu\mu$ + jets data (black), prior to the application of the jet-lepton misidentification probabilities. The central box shows the event selection criteria. The two $WZ \to \mu\nu\mu\mu$ candidates are indicated as stars. The corresponding figures are similar in the channels where the Z boson decays to electrons. There is one candidate for the $WZ \to e\nu ee$ decay channel.

of jet E_T and jet η and are of order 10^{-4}. Applying the misidentification probabilities to jets in the dilepton + jets events yields the total background, estimated to be 0.35 ± 0.02 events. Figure 2 shows the comparison of the dilepton invariant mass and $\not\!\!E_T$ distributions expected for $WZ \to \mu\nu\mu\mu$ events to the background from Z + jets events prior to the folding in of the misidentification probabilities. In $Z + \gamma$ events, a γ may be converted to electrons or randomly match a charged-particle track in the detector causing it to be misidentified as an electron. This background process only contributes to the $e\nu\mu\mu$ and $e\nu ee$ final states. Though we have identified hundreds of $Z + \gamma$ events [23], we found the probability for a photon to be misidentified as an electron is $\sim$2%. As these events do not typically have large $\not\!\!E_T$, the number which mimics the WZ signal is small. We estimate it as 0.145 ± 0.020 events. ZZ events with a lost lepton will appear very similar to the WZ signal. The reconstructed Z bosons are indistinguishable and the average missing transverse energy is only slightly greater. The backgrounds from ZZ and $t\bar{t}$ production are estimated using Monte Carlo methods to be 0.20 ± 0.07 and 0.01 ± 0.01 events, respectively. Other sources of background are found to be negligible. The total background is estimated to be 0.71 ± 0.08 events.

The combination of expected WZ signal and background is consistent with having observed three WZ candidates. The probability for a background of 0.71 events alone to fluctuate to three or more candidates is 3.5%. Following the Bayesian approach outlined in Ref. [22], including Gaussian systematic uncertainties, we obtain $\sigma_{WZ} = 4.5^{+3.8}_{-2.6}$ pb and calculate the 95% C.L. upper limit $\sigma_{WZ} < 13.3$ pb for $\sqrt{s} = 1.96$ TeV.

As σ_{WZ} is consistent with the SM, we can extract limits on anomalous WWZ couplings. Monte Carlo $WZ \to$ trilepton events are generated [24] at each point in a two-dimensional grid of anomalous couplings. We used a parametrized detector simulation to model the detector response and applied the same selection criteria that were applied to the data to determine the predicted WZ signal at each grid point. These predictions are combined with the estimated background and compared with the three observed trilepton candidates to construct a likelihood function L. Analyses of contours of L then permit limits to be set on λ_Z, Δg_1^Z, and $\Delta\kappa_Z$, both individually and in pairs, where $\Delta\kappa_Z \equiv \kappa_Z - 1$ and $\Delta g_1^Z \equiv g_1^Z - 1$. Table II lists one-dimensional 95% C.L. limits on λ_Z, Δg_1^Z, and $\Delta\kappa_Z$ with $\Lambda = 1$ TeV or $\Lambda = 1.5$ TeV. Figure 3 shows two-dimensional 95% C.L. contour limits for $\Lambda = 1.5$ TeV with the assumption of $SU(2)_L \otimes U(1)_Y$ gauge invariance relating the couplings [8]. The values of the form factors are chosen such that the coupling limit contours are within the contours provided by S-matrix unitarity [25].

In summary, we searched for WZ production in $p\bar{p}$ collisions at $\sqrt{s} = 1.96$ TeV. In a sample of 0.30 fb^{-1}, three candidate events were found with an expected background of 0.71 ± 0.08 events. The 95% C.L. upper limit for the WZ cross section is 13.3 pb. Interpreting the candidates as a combination of WZ signal plus background, we find $\sigma_{WZ} = 4.5^{+3.8}_{-2.6}$ pb and provide the first measurement of the WZ production cross section at hadron colliders. We used the results of the search to obtain the tightest available limits on anomalous WWZ couplings derived from a WZ final state. Furthermore, these are the most restrictive model-independent WWZ anomalous coupling limits available and represent an improvement by a factor of 3 over the previous best results [9].

TABLE II. One-dimensional 95% C.L. intervals on λ_Z, Δg_1^Z, and $\Delta\kappa_Z$. In the missing last entry, the 95% C.L. limit exceeded the bounds from S-matrix unitarity. The assumption $\Delta g_1^Z = \Delta\kappa_Z$ is equivalent to that used in Ref. [8].

Condition	$\Lambda = 1$ TeV	$\Lambda = 1.5$ TeV
$\Delta g_1^Z = \Delta\kappa_Z = 0$	$-0.53 < \lambda_Z < 0.56$	$-0.48 < \lambda_Z < 0.48$
$\lambda_Z = \Delta\kappa_Z = 0$	$-0.57 < \Delta g_1^Z < 0.76$	$-0.49 < \Delta g_1^Z < 0.66$
$\lambda_Z = 0$	$-0.49 < \Delta g_1^Z = \Delta\kappa_Z < 0.66$	$-0.43 < \Delta g_1^Z = \Delta\kappa_Z < 0.57$
$\lambda_Z = \Delta g_1^Z = 0$	$-2.0 < \Delta\kappa_Z < 2.4$	—

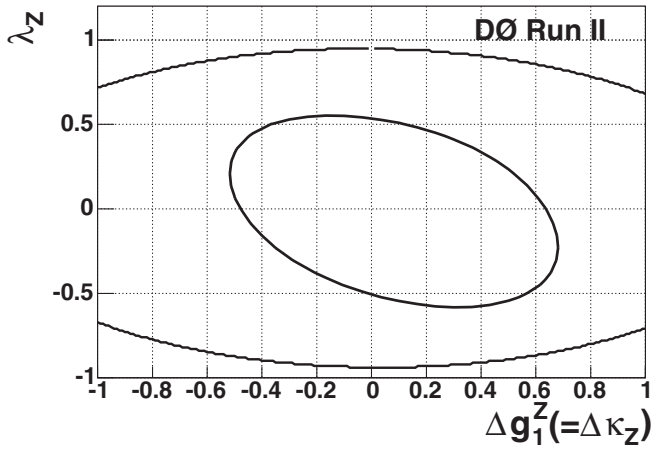

FIG. 3. Two-dimensional coupling limits (inner contour) on λ_Z vs Δg_1^Z at 95% C.L. for $\Lambda = 1.5$ TeV under the assumptions of Ref. [8], which reduce to $\Delta\kappa_Z = \Delta g_1^Z$ for WZ production. The outer contour is the limit from S-matrix unitarity.

We thank the staffs at Fermilab and collaborating institutions, and acknowledge support from the DOE and NSF (USA), CEA and CNRS/IN2P3 (France), FASI, Rosatom and RFBR (Russia), CAPES, CNPq, FAPERJ, FAPESP and FUNDUNESP (Brazil), DAE and DST (India), Colciencias (Colombia), CONACyT (Mexico), KRF (Korea), CONICET and UBACyT (Argentina), FOM (The Netherlands), PPARC (United Kingdom), MSMT (Czech Republic), CRC Program, CFI, NSERC and WestGrid Project (Canada), BMBF and DFG (Germany), SFI (Ireland), A. P. Sloan Foundation, Research Corporation, Texas Advanced Research Program, Alexander von Humboldt Foundation, and the Marie Curie Fund.

*Visitor from University of Zurich, Zurich, Switzerland.

[1] K. Hagiwara, R. D. Peccei, D. Zeppenfeld, and K. Hikasa, Nucl. Phys. **B282**, 253 (1987). There are similar couplings g_1^γ, λ_γ, and $\Delta\kappa_\gamma$ that describe the $WW\gamma$ vertex. Since tree-level unitarity restricts the anomalous couplings to their SM values at asymptotically high energies, each of the couplings must be modified by a form factor, e.g., $\lambda_Z(\hat{s}) = \lambda_Z/(1 + \hat{s}/\Lambda^2)^2$, where $\hat{s}$ is the square of the invariant mass of the WZ system and Λ is the form factor scale.

[2] Kenneth Lane and Stephen Mrenna, Phys. Rev. D **67**, 115011 (2003).

[3] F. Abe *et al.* (CDF Collaboration), Phys. Rev. Lett. **78**, 4536 (1997).

[4] S. Schael *et al.* (ALEPH Collaboration), Phys. Lett. B **614**, 7 (2005).

[5] P. Abreu *et al.* (DELPHI Collaboration), Phys. Lett. B **502**, 9 (2001).

[6] P. Achard *et al.* (L3 Collaboration), Phys. Lett. B **586**, 151 (2004).

[7] G. Abbiendi *et al.* (OPAL Collaboration), Eur. Phys. J. C **33**, 463 (2004).

[8] D. Abbaneo *et al.* (LEP Electroweak Working Group), hep-ex/0412015. They parametrize WWZ couplings in terms of the $WW\gamma$ couplings: $\Delta\kappa_Z = \Delta g_1^Z - \Delta\kappa_\gamma \tan^2\theta_W$ and $\lambda_Z = \lambda_\gamma$.

[9] B. Abbott *et al.* (D0 Collaboration), Phys. Rev. D **60**, 072002 (1999). This Letter contains both a description of a search for $WZ \to$ trileptons with anomalous WWZ coupling limits and a search for non-standard-model $WW + WZ \to \ell\nu$ jet jet production with limits on anomalous $WW\gamma$ and WWZ couplings.

[10] K. Hagiwara, S. Ishihara, R. Szalapski, and D. Zeppenfeld, Phys. Rev. D **48**, 2182 (1993). They parametrize WWZ couplings in terms of the $WW\gamma$ couplings: $\Delta\kappa_Z = \Delta\kappa_\gamma(1 - \tan^2\theta_W)/2$, $\Delta g_1^Z = \Delta\kappa_\gamma/(2\cos^2\theta_W)$, and $\lambda_Z = \lambda_\gamma$.

[11] J. M. Campbell and R. K. Ellis, Phys. Rev. D **60**, 113006 (1999); (private communication).

[12] D. Acosta *et al.* (CDF Collaboration), Phys. Rev. D **71**, 091105 (2005).

[13] S. Abachi *et al.*, Nucl. Instrum. Methods Phys. Res., Sect. A **338**, 185 (1994).

[14] V. M. Abazov *et al.* (to be published); T. LeCompte and H. T. Diehl, Annu. Rev. Nucl. Part. Sci. **50**, 71 (2000).

[15] T. Edwards *et al.*, Fermilab Report No. FERMILAB-TM-2278-E, 2004 (unpublished).

[16] V. M. Abazov *et al.*, Phys. Rev. Lett. **94**, 151801 (2005).

[17] V. M. Abazov *et al.*, Phys. Rev. D **71**, 091108(R) (2005).

[18] S. Abachi *et al.*, Phys. Rev. Lett. **75**, 1023 (1995).

[19] We use a right-handed coordinate system with $\hat{z}$ pointing in the direction of the proton beam and $\hat{y}$ pointing upwards.

[20] T. Sjöstrand *et al.*, Comput. Phys. Commun. **135**, 238 (2001).

[21] R. Brun *et al.*, CERN Report No. CERN-DD-78-2-REV, 1994 (unpublished).

[22] K. Hagiwara *et al.* (Particle Data Group), Phys. Rev. D **66**, 010001 (2002).

[23] V. M. Abazov *et al.* (DØ Collaboration), Phys. Rev. Lett. **95**, 051802 (2005).

[24] K. Hagiwara, J. Woodside, and D. Zeppenfeld, Phys. Rev. D **41**, 2113 (1990).

[25] U. Baur, hep-ph/9510265.